



# Durability of photocatalytic ZnO-based surface coatings and preservation of their antibacterial effect after simulated wear

Mati Kook, Harleen Kaur, Dmytro Danilian, Merilin Rosenberg, Vambola Kisand, Angela Ivask 

Received: 29 July 2023 / Revised: 6 October 2023 / Accepted: 8 October 2023  
© The Authors 2024

**Abstract** This study focused on antibacterial durability testing of surface coatings based on acrylic matrix-embedded UVA-activated ZnO. Such coatings on stainless steel were treated by dry rubbing, wet rubbing, and abrasive treatment to simulate wearing during everyday touching, cleaning, and aggressive scrubbing. Abrasive treatment caused clear topological changes to the surfaces, flattened the surface at the micrometer scale, and released a significant amount of surface material, which was partly acrylic matrix and partly the embedded ZnO. The highest release of Zn, the most prominent photocatalytic activity under UVA and the greatest antibacterial effect, was observed for abrasively treated surfaces. Although a small amount of surface material was released from surfaces after dry and wet rubbing, no significant increase in Zn release or photocatalytic activity was detected. On the contrary, antibacterial activity after those treatments decreased in comparison with untreated surfaces, likely due to partial surface masking by the released acrylic matrix. In summary, our results indicate that antimicrobial ZnO material immobilized in acrylic matrix creates stable surface coatings that may lose some of their efficacy during

daily use and cleaning procedures, but activity of which will be retained during a more aggressive abrasion procedure.

**Keywords** ZnO, Acrylic matrix, Antimicrobial efficacy, Photocatalytic activity, Stability

## Introduction

High-touch surfaces have been considered as an important source of infectious disease outbreaks.<sup>1</sup> Even up to 40% of microbial infections in hospital settings may spread through fomites or microbe-contaminated materials.<sup>2,3</sup> Therefore, introduction of antimicrobial coatings on surfaces at infection hot spots to prevent adhesion, proliferation, or decrease residence time of microbes, would potentially provide socioeconomic and health benefits.<sup>4</sup> In most studies, the efficacy of antimicrobial coatings in reducing microbial bioburden has been clearly demonstrated in laboratory model conditions, on newly prepared surfaces and in conditions usually not representing the application-relevant use scenarios.<sup>5,6</sup> Only a few studies in which activity of antimicrobial coatings has been shown during their real-life use have been published.<sup>7</sup> Those studies have demonstrated either decrease in surface-residing microbes or related infections after introduction of copper-based surfaces, but reliable data are generally lacking for other types of surfaces.<sup>8,9</sup>

Recent comparisons between the activity of antimicrobial surfaces in standardized test conditions and real-life relevant conditions have indicated that these do not always coincide. Factors such as temperature, relative humidity, and the presence of organic soiling may significantly affect antibacterial activity of the surfaces.<sup>5,10,11</sup> For example, copper-based surfaces that are based on slow release of antimicrobially active copper ions allow the accumulation of dead bacterial

---

**Supplementary Information** The online version contains supplementary material available at <https://doi.org/10.1007/s11998-023-00868-2>.

---

M. Kook, D. Danilian, V. Kisand (✉)  
Institute of Physics, University of Tartu, W. Ostwaldi 1,  
50411 Tartu, Estonia  
e-mail: vambola.kisand@ut.ee

H. Kaur, M. Rosenberg, A. Ivask (✉)  
Institute of Molecular and Cell Biology, University of Tartu,  
Riia 23, 51010 Tartu, Estonia  
e-mail: angela.ivask@ut.ee

biomass that can block ion release and lead to surface inactivation.<sup>12,13</sup> Apart from surface inactivation by dead bacteria, other types of organic material originating from the environment as well as physical aging or chemical changes may also significantly affect the activity of antimicrobial surfaces. However, loss of efficacy over time is an important drawback hindering the use of antimicrobial surfaces in real applications.<sup>14</sup> Despite this, stability and durability in application-relevant conditions and over longer periods of time are properties largely overlooked in most of the studies published thus far on antimicrobial surfaces.<sup>15</sup>

One of the potential issues impeding the durability testing of antimicrobial surfaces is the lack of clear performance criteria and appropriate testing methods. Most articles focusing on stability of surfaces have focused on mechanical durability testing and not specifically on preservation of antimicrobial activity. Accepted durability testing methods include cross-cut method enabling to evaluate adhesion between substrate and coating material, pencil hardness test that estimates mechanical hardness of coating material, TABER<sup>®</sup> rotary platform test that characterizes mechanical abrasion, and impact test that identifies how a coating performs under a rapid deformation process.<sup>16–19</sup> The simplest and most widely used mechanical wear testing method involves sandpaper abrasion with specified weight, fixed speed, and distance.<sup>20–22</sup> On the other hand, no widely used methods exist for evaluation of stability of antimicrobial effect of surfaces, and only a limited number of publications are available on that topic. One of the simplest methods that has been used involves consecutive antimicrobial tests alternating with simple rinsing. Such method has been used to demonstrate the preservation of photoactivated antimicrobial effect of ZnO/Ag nanocomposite-based surfaces over ten use cycles,<sup>23</sup> as well as to show the silver ion leaching from silver zeolite-coated surfaces over one year.<sup>24</sup> Other studies have followed the guidance for mechanical testing and studied the effect of wiping or abrasion on antimicrobial activity. In those studies, preservation of antibacterial efficacy of zeolite-incorporated silver nanoparticles encapsulated by hydrophilic polymers toward *Escherichia coli* was demonstrated after 1200 repeated dish soap solution wipings, or over 30 wash cycles with artificial sweat,<sup>19</sup> retainment of antibacterial effect of copper nanoparticles containing surfaces after rubbing was shown,<sup>25</sup> and resistance of surfaces with acrylonitrile butadiene styrene plastic-immobilized TiO<sub>2</sub> nanoparticles to wiping, brushing, and scratching was proven.<sup>26</sup> At the same time, if TiO<sub>2</sub> nanoparticles were simply electrosprayed to surface, poor wiping and abrasion durability were measured.<sup>26</sup> A rubbing procedure has been also shown to significantly decrease the activity of plastic surfaces containing immobilized tributyl phosphonium compounds against *Arthrobacter* and *E. coli*, whereas plastic surfaces coated with perfluoroalkyl compound retained its antibacterial activity.<sup>27,28</sup> Also, peeling tests have been used to demonstrate the mechanical antibacterial durability of zwitterionic copolymers

and silver-based surface coatings.<sup>29,30</sup> As a more aggressive treatment, ultrasonication of surfaces has been applied, and copolymer-embedded zwitterionic material was shown even to resist such treatment.<sup>29</sup> One of the methods suggested by the US EPA Office of Pesticide Programs to be used to test the preservation of antimicrobial effect of surfaces is US EPA Interim Guidance for Evaluating the Efficacy of Antimicrobial Surface Coatings that involves suggestions for testing of durability to both physical and chemical treatments and enables the durability for maximally over four weeks.<sup>31</sup> Following this guidance, antiviral durability of organosilane quaternary ammonium compound-based coatings and two commercial “peel and stick” coatings was studied and the results showed that most of the tested surfaces lost their activity during the procedure and thus are not expected to resist routine cleaning, disinfection with chemicals, or potentially simply wetting the treated surfaces.<sup>32</sup>

Despite its importance, antimicrobial durability testing is not frequently discussed in research papers concerning antimicrobial surfaces and thus, many initially promising surfaces may not be robust enough to survive the proposed end-application. A general search from ISI Web of Science showed that only around 1% of all 40,000 publications available on search term “antimicrobial AND surface\*,” may also contain information on some aspects of durability. Moreover, as preservation of antimicrobial activity is evidently dependent on the surface or its coating properties as well as on the testing method, each proposed antimicrobial surface should undergo application-relevant durability testing. In this study, we evaluated the effect of three treatments on antimicrobial performance of UVA-activated photocatalytic surface coatings that are based on acrylic polymer matrix-immobilized ZnO micro- and nanostructures and applied onto stainless steel surface.<sup>23,33</sup> Such surfaces have the potential to be used outdoors or by sunlight well-illuminated indoor conditions and therefore, their exposure to various wear and tear is a realistic scenario. Two of the applied treatment methods followed the suggestions of the US EPA method for antimicrobial surfaces and modeled daily abrasive wearing and wet cleaning process, and one applied method involved abrasion, expected to model extreme abrasion, e.g., by scraping.<sup>31</sup> Post-treatment physical changes of the surface coatings were described, release of Zn as the active component was analyzed, and photocatalytic and antimicrobial activity of the surface coatings was determined. We expected the study to provide information on durability of photocatalytically active antibacterial surfaces during different use scenarios.

## Materials and methods

For all experiments, type II deionized water (Pacific TII Water Purification System) was used. The following key chemicals were used for chemical synthesis:

methanol (Sigma-Aldrich, puriss,  $\geq 99.8\%$ ), 1-butanol (Sigma-Aldrich, puriss,  $\geq 99.5\%$ ), KOH (LACH-NER, 90.0%), and  $\text{Zn}(\text{CH}_3\text{CO}_2)_2$  (Sigma-Aldrich,  $\geq 99.0\%$ ). All other chemicals were of analytical grade. Ultrasonic bath Elma Elmasonic P 30 H (max. power 320 W) or ultrasonic homogenizer UP200Ht Sonotrode S26d7D with titanium probe and maximal output 200 W (Hielscher Ultrasonics) were used throughout the study.

### Preparation of ZnO micro- and nanocomposite-based surface coatings

AISI304L stainless steel (SS) disks (Outokumpu, Finland, 8% Ni, 18% Cr, 75% Fe, 2B surface finish) that were laser cut to 20-mm diameter and had thickness of 2 mm were used as substrates. Prior to applying the ZnO-based coatings, the disks were cleaned with water and Fairy washing liquid (1 drop in 400 mL of water; Procter and Gamble) followed by 3 times water rinse. Then, the disks were cleaned in an ultrasonic bath for 15 min in 400 mL of water, for 15 min in 400 mL of acetone, for 15 min in 400 mL of water, for 15 min in 400 mL of ethanol, and for 15 min in 400 mL of water. Finally, SS disks were dried at ambient conditions.

Two types of ZnO (Supplementary Fig. S1) were used to prepare coatings onto SS disks: commercial ZnO (color pigment Sennelier Zinc White, color code PW4, Max Sauer SAS, France) with microsize irregular-shaped particles, approximately 500–2000 nm in diameter, designated as ZnO(c), and in-house synthesized ZnO with 20 nm (diameter)  $\times$  120 nm (length)-sized nanorods designated as ZnO(s). The in-house synthesis protocol and the resulting ZnO(s) nanostructures have been described in detail in our previous study.<sup>33</sup> The acrylic polymer chosen as a matrix for ZnO nanostructures was two-component matte topcoat from SIRCA S.p.A, Italy (topcoat F40P005, aliphatic hardener F901CT and thinner DT452) designed for metal surfaces. First, 56 wt% topcoat and 14 wt% hardener were mixed by a vortex mixer. To that, 30 wt% of thinner (in the case of samples without ZnO, designated as matrix, *M*) or thinner previously mixed with ZnO was added, and mixed again. In the case of ZnO samples, ZnO(c) or ZnO(s) nanostructures were mixed with topcoat thinner using wt ratio 92:8 thinner/ZnO, dispersed using ultrasonic homogenizer for 5 min (in regime 0.5 s ultrasonic, 0.5 s switched off, and amplitude 33%) and additionally vortexed for 10 s. The resulting mixtures were then added to topcoat and hardener mixture as described above. SS disks were coated with the mixtures: acrylic topcoat mixed with pure thinner, thinner supplemented with ZnO(c), or ZnO(s) to produce matrix only (*M*), ZnO(c), or ZnO(s) surfaces. Next, 70  $\mu\text{L}$  of the mixtures was pipetted onto a SS disk on a self-made rotating spin coater, which was turned on to 300 rpm for 3 s. After coating, SS disks were dried for 24 h at room temperature laboratory conditions.

### Treatment of coated surfaces for simulated wear

Three different treatments were performed to evaluate the durability of ZnO micro- and nanostructures-based surface coatings after simulated wear. A custom automated abrasion tester based on open-source RepRap hardware and software (reprap.org) was used for all treatments. Two of those dry and wet rubbing methods followed EPA Interim Guidance for Evaluating the Efficacy of Antimicrobial Surface Coatings.<sup>31</sup> For dry (D) rubbing, a sponge (Scotch Brite Non-Scratch Scrub Sponge, length 9.2 cm) with its nonabrasive side and with additional weight of 224 g was used. The sponge was passed over coated surfaces for 40 cycles, each cycle consisting of 16 passes (8 passes over the disk back and forth) and each pass lasting for 2.5 s (38 cm horizontal movement for one-way shift). Between every cycle, there was 20 min waiting time. The used 40 treatment cycles correspond to a 4-week long-use claim according to EPA guidance.<sup>31</sup> For wet rubbing (W), the procedure described above was amended with a 2000 mg/L of NaOCl chosen as a commonly used chemical disinfectant. Then, 20 mL of NaOCl solution was poured onto the bottom of the dish, and the sponge was soaked there for a minimum of 10 min prior to passing it over the coated surfaces with an additional weight of 454 g. Pass length and moving speed were the same as in the case of D treatment, but one cycle consisted of 8 passes (4 passes over the disk back and forth). After every cycle, 30 min waiting time was used. A new sponge was replaced after every 5 cycles. A total of 40 cycles were completed, which according to EPA guidance is equivalent to a 4-week claim.<sup>31</sup>

The third treatment was based on sandpaper abrasion protocol that is a common method used to test mechanical properties of surfaces and has generally been expected to remove the topmost layer of coatings.<sup>21</sup> For this, 10-cm-long abrasive pad with 3000 grit (surface structure shown on Fig. S2, 3M™ 443SA Trizact™ Fine Finishing Disk, silicon carbide) using additional weight of 100 g was passed over coated surfaces. The pass length and speed matched those of D and W, and 100 consecutive passes were performed. Surfaces treated using this process are marked with A (abrasion).

D, W, and A treatments were performed for every surface coating type, *M*, ZnO(c), and ZnO(s). All the different variants of surfaces and their treatments are shown in Supplementary Table S1.

### Photocatalytic activity measurement

Photocatalytic activity was measured on the basis of methylene blue (MB) degradation. The coated surfaces were placed into wells of 6-well microplates, 5 mL of  $1.0 \times 10^{-5}$  M MB aqueous solution was pipetted into each well, and the whole plate was covered with UV transparent borosilicate glass to suppress evaporation.

Into each well, magnetic stirring bar ( $7 \times 2$  mm) was placed and stirring at 150 rpm was carried out during the whole experiment. To decrease drying effects, all photocatalytic experiments were performed in a pre-conditioned climatic chamber (Memmert CTC 256, Germany) at 23°C and 90% relative humidity (RH).

A self-built lamp consisting of four fluorescent Hg light bulbs (15 W iSOLde Cleo,  $\lambda_{\max} = 355$  nm) was used, and the light intensity at test surface height was 2.4–3.0 W/m<sup>2</sup> at 315–400 nm spectral range (i.e., in the UVA region, measured using Delta Ohm UVA probe through borosilicate cover glass). The pH of the initial MB solution was 7.0. Degradation of MB was measured in 4 parallels. Degradation of MB solution with working stirrer but without sample measured under the same conditions served as reference. Before experiments, the samples with dye solution were pre-conditioned for 20 min in dark to establish the adsorption equilibrium of MB. After the degradation experiment, the MB solution was poured into a standard PS 10-mm optical length cuvette to measure the UV–Vis absorbance of MB using a spectrophotometer (Agilent Cary UV–Vis-NIR 5000, Agilent, USA). The absorbance intensity at 663 nm (characteristic absorbance peak for MB) after the test was compared to the initial intensity to evaluate the degradation of MB.

### Scanning electron microscopy imaging

Scanning electron microscope (SEM) Nova NanoSEM 450 with 3 kV electron acceleration voltage and secondary electron detector was used to visualize the top view of all the coatings. Samples were placed on the SEM stub with carbon tape. In all cases, nonconducting surfaces were covered with a 6-nm layer of gold. All sample types were imaged in SEM in 1000 $\times$ , 10,000 $\times$  and 100,000 $\times$  magnifications to detect morphological changes in the surface layer of the coating after simulated wear. The 1000 $\times$  fields were chosen randomly and 10,000 $\times$  fields were captured of protruding features of the acrylic coating, visible signs of morphological changes and low areas where debris had accumulated. The images were captured and presented for illustrative purposes, and no SEM image analysis techniques were used.

### Contact angle measurements

The sessile drop method was used to measure surface water drop contact angles using a moving platform based on Thorlab DT12 (Newton, NJ, USA) dovetail translation stage.<sup>34</sup> A 2  $\mu$ L drop of deionized water was pipetted onto each coated surface. After 10 s, the water droplet was photographed with a Canon EOS 650d camera (Ota City, Tokyo, Japan) using a MP-E 65 mm f/2.8 1–5  $\times$  Macro focus lens. Image analysis

software (ImageJ 1.8.0 172 [NIH, Madison, WI, USA] for Windows, plugin for contact angle measurement) was used to determine the contact angle formed by the liquid drop on the glass surface.<sup>35</sup> The average of contact angles measured from four water droplets per sample was calculated. Samples with contact angle  $< 90^\circ$  were considered hydrophilic, and samples with contact angle  $> 90^\circ$  were considered hydrophobic.<sup>36</sup>

### Determination of Zn release from surfaces

To measure the release of Zn, 500  $\mu$ L of deionized water was placed onto each surface so that the liquid covered the surface maximally. The surface was incubated at room temperature for 4 h, and maximal volume of liquid was removed. For each analysis, four surfaces were pooled to obtain an average Zn concentration. Prior to the measurement appropriate dilutions of the samples were made. ICP-MS (Agilent 7700) measurement of Zn concentration in the water samples were performed following the ISO 17294-2:2016 standard.<sup>37</sup>

### Antibacterial activity evaluation

Antibacterial activity of coated surfaces was evaluated against Gram-negative *Escherichia coli* DSM 1576 (ATCC 8739) using a microdroplet method.<sup>10</sup> Bacteria were grown overnight on LB agar (5 g/L NaCl, 10 g/L tryptone, 5 g/L yeast extract, and 15 g/L agar) plates, collected using a sterile inoculation loop to prepare the inoculum in 500-fold diluted Nutrient Broth (0.006 g/L meat extract, 0.02 g/L peptone, and 0.01 g/L NaCl). Alternatively, for testing of wet rubbed (W) surfaces, bacterial inoculum was prepared in 500-fold diluted Nutrient Broth that was supplemented with 0.5 g/L of Na<sub>2</sub>S<sub>2</sub>O<sub>3</sub> to neutralize mainly the effect of chlorine residues that may be present on wet rubbed surfaces after sodium hypochlorite treatment.<sup>38</sup> The cell density was adjusted photometrically to achieve a target OD<sub>600</sub> value of 0.074, corresponding to approximately  $1.05 \times 10^8$  CFU/mL. The surfaces were inoculated with  $5 \times 2$   $\mu$ L microdroplets of the bacterial inoculum and placed in a closed Petri dish system to minimize ventilation effects on inoculum drying. Surfaces were then incubated in a climate chamber (Climacell EVO, Memmert, USA) at 90% relative humidity and 22°C for 4 h. Exposures were conducted in parallel in the dark or under UVA illumination, in which case a 1.1-mm-thick UVA-transmissive borosilicate moisture preservation glass was used as a cover. For UVA, UVA/Vis Combi light tray of the climate chamber was used, and UVA intensity was measured 2.0 W/m<sup>2</sup> at 315–400 nm spectral range. After the exposure, surfaces were placed to tubes containing 10 mL of SCDLP toxicity neutralizing medium (17 g/L casein peptone,



3 g/L soybean peptone, 5 g/L NaCl, 2.5 g/L Na<sub>2</sub>HPO<sub>4</sub>, 2.5 g/L glucose, 1.0 g/L lecithin, and 7.0 g/L Tween 80) and vortexed for 30 s to detach the bacteria.<sup>39</sup> Serial tenfold dilutions in phosphate-buffered saline (PBS: 8 g/L NaCl, 0.2 g/L KCl, 1.44 g/L Na<sub>2</sub>HPO<sub>4</sub>, 0.2 g/L KH<sub>2</sub>PO<sub>4</sub>; pH 7.1) were made and 20 µL of the dilutions were drop-plated on LB solid medium (5 g/L yeast extract, 10 g/L tryptone, 5 g/L NaCl, and 15 g/L agar). Plates were then incubated for 16–18 h at 37°C, viable counts as colony-forming units (CFU) were counted, and results were expressed as log<sub>10</sub>-transformed CFU counts per surface. The theoretical limit of detection (LOD) was calculated using the value of 3 colonies × dilutions of the final culture. For statistical analysis, all CFU values below LOD were adjusted to LOD. All antibacterial testing experiments were conducted in at least three biological replicates with two technical replicates.

### Statistical analysis

Statistical analysis of the data was performed with GraphPad Prism 9.5.0 (GraphPad Software, San Diego, USA). Raw data used can be found in the Supplementary Raw Data file. One-way ANOVA followed by Tukey's multiple comparisons test at  $\alpha = 0.05$  was used where appropriate.

## Results and discussion

### Physical changes of surface coatings during simulated wear

SEM images of the studied surfaces (Fig. 1) indicated that the newly prepared acrylic matrix or ZnO-containing acrylic matrix coating on stainless steel appeared smooth but not totally flat as expected from a matte surface topcoat. No visible ZnO particles extruded from the topmost layer in the case of ZnO-containing surface coatings and thus, we conclude that the top layer of the surface coating was matrix polymer. Similar smooth surface structures have been previously shown for Aeroxide® TiO<sub>2</sub> P25 nanoparticles-based acrylic paint on wooden substrate.<sup>40</sup> This observation is in good agreement with the general idea that smoothness of polymer surfaces depends strongly on pigment/polymer ratio, and in the case of low pigment/polymer ratio, obtained surfaces are rather smooth.<sup>41</sup>

All the wear-simulating treatment procedures used, however, introduced clear changes to all the surface coatings. Already at 1000× magnification under SEM, clear changes were observed for samples treated by abrasion (Figs. 1a–c, upper rows). Visible scratching marks appeared, and a part of the topmost matrix polymer was removed from higher structures, thereby flattening the initial surface coating. The topographical

structure of the abrasive pad is presented in Supplementary Fig. S2, and it is clear that the scratching marks on surface (red arrows on Fig. 1) represent traces of the structures of this abrasive pad. At 10,000× magnification SEM images, changes of surface coatings were observed for every treatment (Figs. 1a–c, lower rows). Solid material that was either acrylic matrix polymer or embedded ZnO micro- and nanostructures was released and accumulated either near the edges of the higher structures in the case of dry rubbing (D) or spread over the whole surface in the case of wet rubbing (W) (Supplementary Fig. S3). However, interestingly, the appearance of scratching marks and release of surface material did not affect surface hydrophobicity as evidenced by contact angle measurements (Fig. 2). The contact angles of all the surface treatment types were statistically similar, > 90° and thus, were classified hydrophobic.<sup>36</sup> It is well-known that hydrophobic/hydrophilic properties of surfaces are influenced by both topographical structure and chemical composition of surface. Since our experiments do not influence contact angle even in the case of abrasion, it is reasonable to conclude that hydrophobic/hydrophilic properties in the case of present surfaces are dominated by the chemical composition of surface.

In addition to topographic characterization, the surface coatings were also characterized for their Zn release profile. Although both ZnO(c) microstructures and ZnO(s) nanostructures were fully immobilized into the acrylic topcoat matrix, release of Zn ions was still possible due to low level surface leaching or minor release of ZnO particles. Such release was expected to be very low in the case of untreated samples as the topmost surface was dominated by acrylic polymer matrix (Fig. 1a). However, as release of solid material was observed from the topmost layer of ZnO(c) and ZnO(s) surface coatings (Supplementary Fig. S3), liberation of either ZnO particulates or Zn ions was expected to increase. Such an increased release of Zn from surfaces may however play an important role in antimicrobial activity as both liberated Zn ions as well as ZnO particles may exert antibacterial activity and additionally, released ZnO particles may contribute to photocatalytic effect. It is important to note that Zn release experiments could not be conducted exactly at conditions mimicking antibacterial or photocatalytic measurements due to their too low liquid content (antibacterial tests) or too high dilution (photocatalytic activity measurement). Therefore, the results on Zn release profiles are comparable between sample and treatment types and are not exactly transferrable to antibacterial or photocatalytic tests. In parallel to ZnO surfaces, released Zn was also quantified from matrix only covered surfaces, where Zn content was 17.5 ng/surface (marked to Fig. 3 with dashed line). Detectable amounts of Zn were released from ZnO-containing surfaces either in the form of Zn ions or ZnO particulates. In general, ZnO(s) nanostructures-based surfaces released less Zn than ZnO(c)

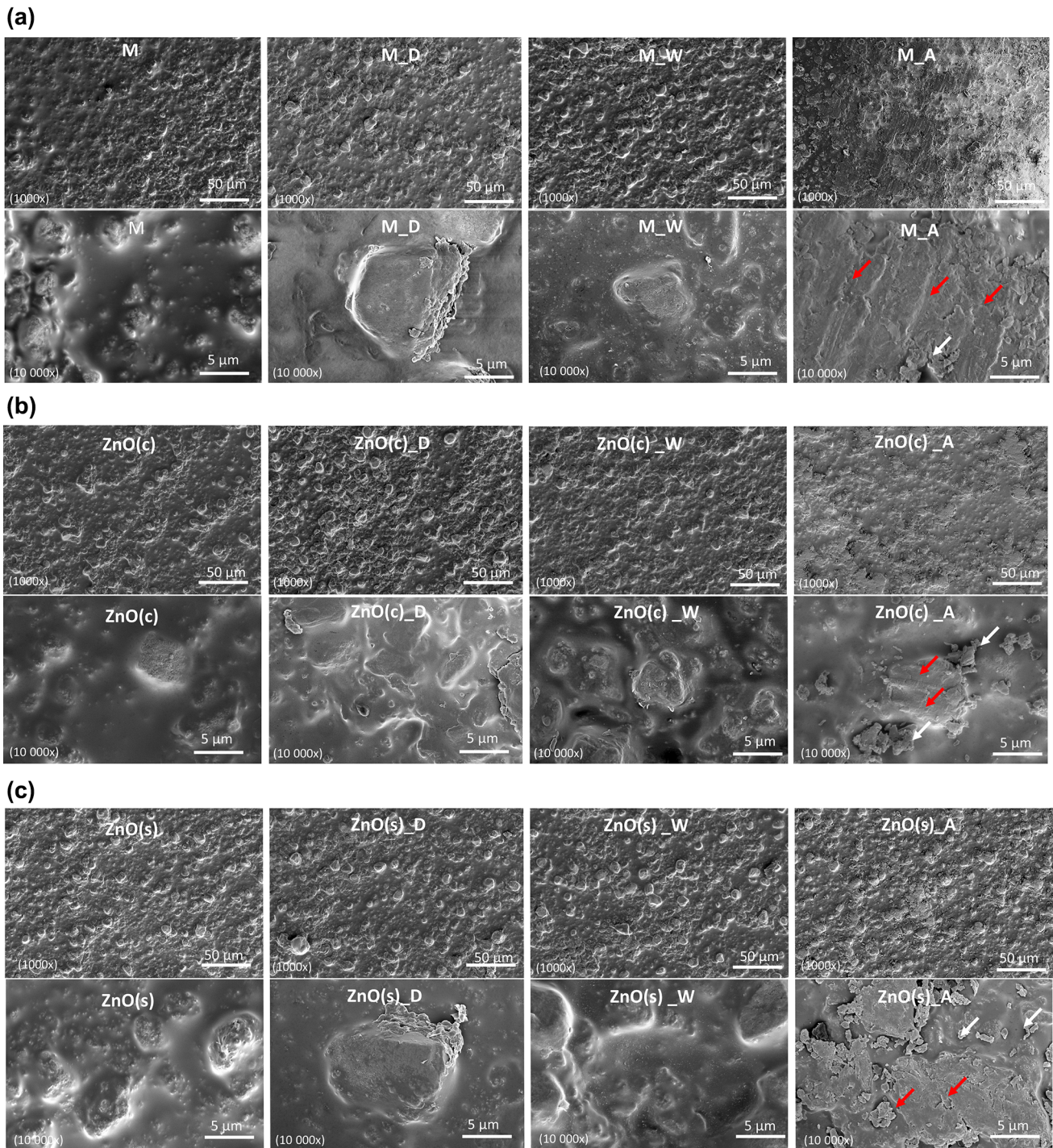


**Fig. 1: SEM images of surface coatings. (a) Acrylic topcoat matrix covered surfaces, (b) ZnO(c) in acrylic topcoat matrix surfaces, (c) ZnO(s) in acrylic topcoat matrix surfaces. Untreated surfaces (left column) and surfaces treated with dry (D) or wet (W) rubbing and abrasive treatment (A) procedures were viewed using 1000× [upper rows of (a)–(c)] and 10,000× [lower rows of (a)–(c)] magnification. Red arrows indicate visible scratches and white arrows indicate released surface coating material**

microstructures-based surfaces, and more Zn was released under UVA treatment than in dark (Fig. 3a, b). Dry (D) and wet (W) rubbing did not notably affect surface release of Zn but surfaces after abrasive

treatment (A) released considerably higher amounts of Zn. This observation is in correlation with SEM images demonstrating visible physical changes on ZnO-containing surfaces and release of surface coating



material (Fig. 1b, c). Thus, we can conclude that zinc as active ingredient is released from ZnO-containing surfaces, and its release is significantly increased after abrasive treatment. This released fraction of Zn may further contribute to both antimicrobial as well as to photocatalytic activity of ZnO-based surfaces. To the best of our knowledge, similar release experiments with high sensitivity chemical methods have not been reported in the literature in the case of ZnO-containing acrylic surfaces or paints.

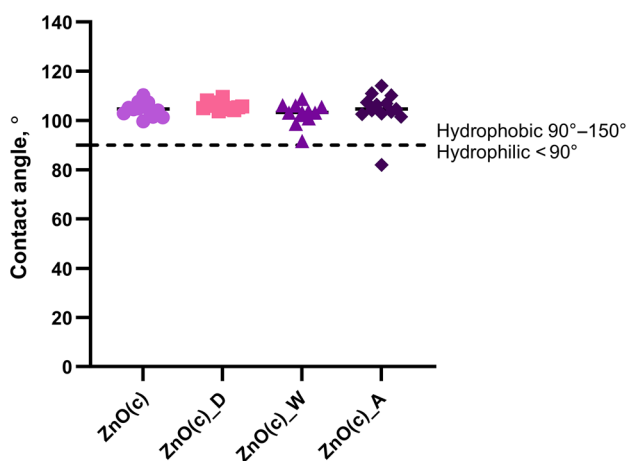
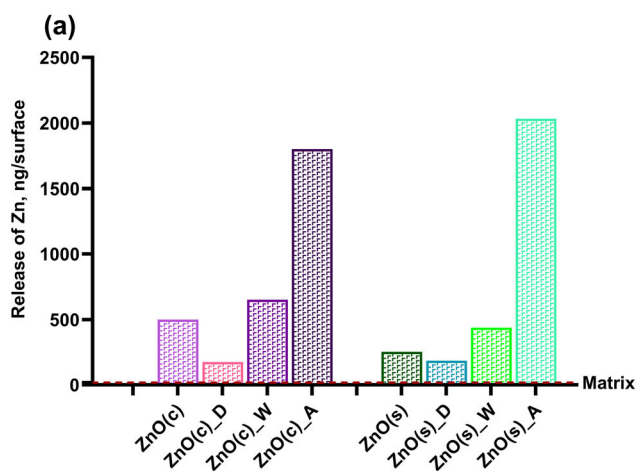


**Fig. 2: Contact angles of surface coatings before and after treatment.** ZnO(c) in acrylic matrix surfaces were used as model surface in untreated form or after dry (D) or wet (W) rubbing, or abrasive treatment (A). Single measurement values and average are shown. The dashed line represents 90° contact angle above which surfaces were considered hydrophobic



**Photocatalytic activity of surface coatings after simulated wear**

Due to the photoinduced nature of ZnO and formation of reactive oxygen species during exposure of ZnO to UVA, the effect of wear-simulating surface treatments on photocatalytic activity of ZnO-based surface coatings was studied.<sup>42</sup> Methylene blue (MB) was used as a photocatalytically degradable model dye and disappearance of the dye after exposure to the different samples was measured (Fig. 4). As expected, none of the samples exhibited notable photocatalytic activity in the dark (Fig. 4b). Under UVA, however, ZnO-based surface coatings showed significant photocatalytic effect (Fig. 4a). There was no significant difference between photocatalytic activity of surfaces containing ZnO(c) microparticles or ZnO(s) nanoparticles. Also, matrix alone showed some photocatalytic effect under UVA, which was probably caused by light-aided degradation of MB dye. However, this effect was significantly lower than the effect of ZnO-based surface coatings. Significant photocatalytic effect of ZnO-based surface coatings has also been demonstrated in earlier studies, where ZnO powder was immobilized to acrylic paint, mostly for decoration of indoor surfaces.<sup>43,44</sup> Similar to our study, Vu et al. showed that while both ZnO nanoparticle- as well as microparticle-based coatings exhibited photocatalytic activity, weak photocatalytic effect was observed also in the case of neat coatings.<sup>44</sup>

Among the used surface treatment methods, only abrasive treatment had a notable effect on photocatalytic activity of the ZnO-based surface coatings (Fig. 4a, c). The photocatalytic activity of both ZnO(c) and ZnO(s)-based coatings significantly increased after abrasive treatment. At the same time, dry and wet rubbing had no significant effect on MB degradation profile of any of the surface coatings. This finding is in

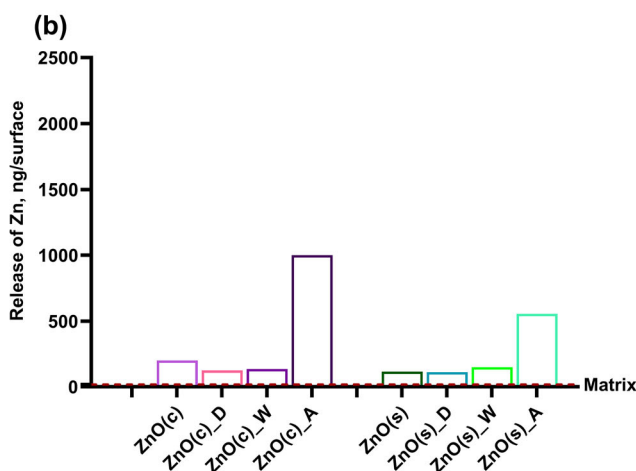


**Fig. 3: Release of Zn from surface coatings before and after treatment.** Release of Zn was measured over 4 h under UVA illumination (a) or in the dark (b) from ZnO(c) or ZnO(s)-based surface coatings after their dry (D) or wet (W) rubbing, or abrasion (A). The dashed line represents the amount of Zn released from matrix alone surfaces. The values demonstrate the average Zn release measured from four parallels from each treatment group

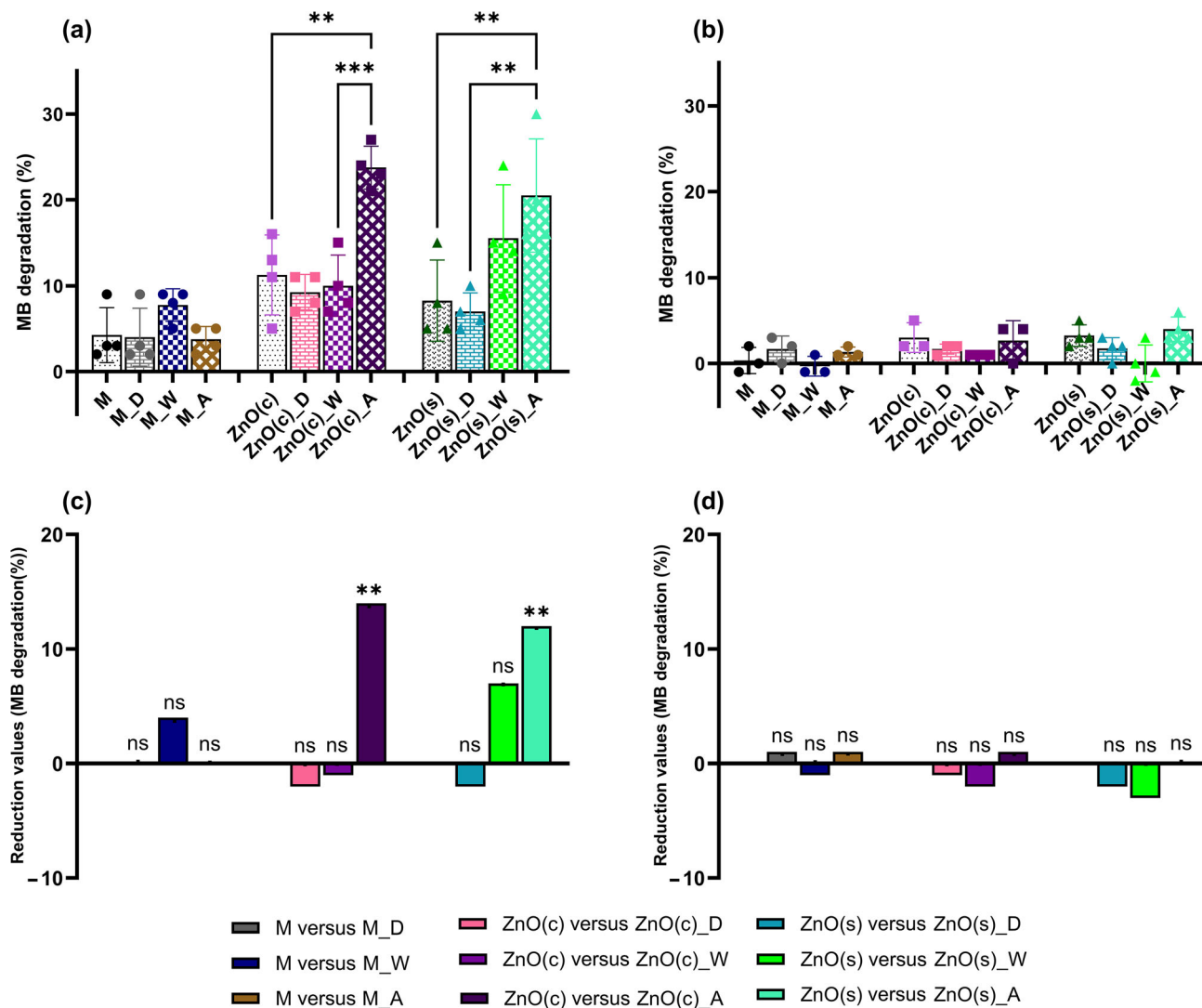


**Fig. 4: Photocatalytic activity of surface coatings before and after treatment. Photocatalytic activity observed as degradation of methylene blue (MB) dye by matrix alone (M), ZnO(c) or ZnO(s) surface coatings after dry (D) or wet (W) rubbing, or abrasive treatment (A). (a) Photocatalytic activity under UVA and (b) photocatalytic activity in dark conditions. Lower panels represent the differences in MB degradation between surfaces treated by D, W, or A and the untreated surface under UVA (c) or in the dark (d). Color codes used on (c) and (d) are shown. Datapoints and average of four parallels with standard deviation are shown. Statistically significant differences ( $p < 0.05$ ) are shown as: ns—nonsignificant, \*\* ( $p < 0.01$ ), \*\*\* ( $p < 0.001$ )**

correlation with previous information on Zn release based on what abrasive treatment released either Zn ions or ZnO particulates, while dry and wet rubbing had no such effect (Fig. 3). Increased photocatalytic activity of abrasively treated ZnO-based surfaces suggests that the material released from such surfaces (see SEM images of A samples on Fig. 1a–c) was mostly photocatalytically active ZnO. Indeed, closer investigation of abrasively treated surfaces revealed the presence of protruding ZnO particulates (Supplementary Fig. 4e, f) that may have exhibited photocatalytic activity. These results suggest that abrasive treatment may effectively enhance the photocatalytic and self-cleaning activity of ZnO-based acrylic matrix

coated surfaces, however at the same time also potentially decrease the lifetime of those surfaces.

#### **Antibacterial activity of surface coatings after simulated wear**

The preservation of antibacterial activity after treatments simulating different wear scenarios was tested with *E. coli*. The bacteria were exposed to surface coatings for 4 h as pilot experiments indicated that longer timepoints than 4.5 h under UVA caused almost full inactivation of surface-exposed bacteria (Supplementary Fig. S4) and thus quantitative com-



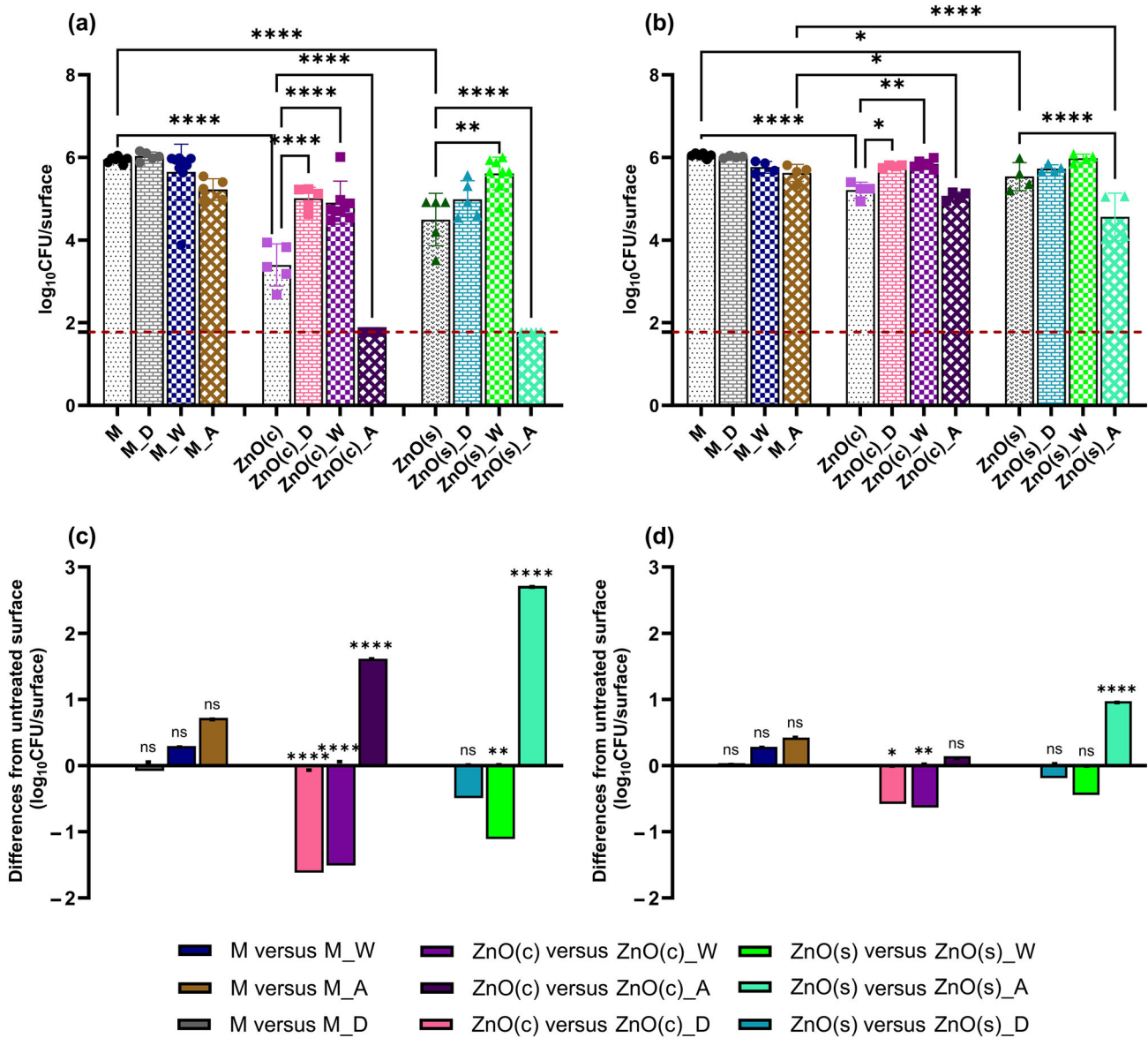


**Fig. 5: Antibacterial activity of surface coatings before and after treatment. The number of  $\log_{10}$  colony forming units (CFU) of *E. coli* per surface of matrix alone (M), ZnO(c), or ZnO(s) after 4 h exposure under UVA (a) or in the dark (b). Surfaces were tested either untreated or after dry rubbing (D), wet rubbing (W), or abrasive (A) treatment. Red dotted line represents the detection limit (LOD). Lower panels represent the differences in antibacterial activity (CFU count per surface) between surfaces treated by D, W, or A and the untreated surface under UVA (c) or in the dark (d). Color codes used on (c) and (d) are shown. Datapoints and average are shown with standard deviation. ns—nonsignificant, \*  $p < 0.1$ , \*\*  $p < 0.01$ , \*\*\*  $p < 0.001$ , \*\*\*\*  $p < 0.0001$**

parison with wear simulated treatments would have been impossible. Exposure of *E. coli* for 4 h to untreated ZnO-containing surface coatings had a statistically significant antibacterial effect both under UVA as well as in the dark (Fig. 5a, b). Under UVA, the untreated ZnO(c) surface coating resulted in 2.5  $\log_{10}$  decrease in viable count and the untreated ZnO(s) surface coating decreased viability by 1.5  $\log_{10}$ . Although those surfaces exhibited statistically significant antibacterial effect also in the dark, this effect had a relatively low biological importance (0.5

$\log_{10}$  decrease in the case of ZnO(c) surface and 0.25  $\log_{10}$  decrease in the case of ZnO(s) surface). This result indicating that the antibacterial potential of ZnO-based surfaces reveals mainly under UVA suggests that the prevailing mode of action of ZnO(c) and ZnO(s) surface coatings was UVA-induced photocatalytic activity and production of reactive oxygen species, as also suggested in previous studies.<sup>45</sup> The statistically significant but biologically less relevant decrease in bacterial viable counts on ZnO(c) and ZnO(s) surfaces in the dark suggested low but existing

antibacterial effect due to surface-released Zn ions or ZnO particulates (Fig. 3).

Interestingly, we observed that wet (W) rubbing of matrix only surfaces caused significant antibacterial activity (Supplementary Fig. S5), which was not only most prominent under UVA illumination, but also detectable in the dark. We suggest that despite careful rinsing with deionized water, remaining residues of hypochlorite cleaning agent were left on W surfaces, and a subsequent exposure of such residues to UVA evoked a synergistic effect between chlorine and short wavelength light. As shown earlier by Blomberg et al., the treatment of surfaces by any cleaning or disinfection agent may leave residues and thus, the potential interference of such residues with antimicrobial efficacy should be accounted for.<sup>46</sup> Also, the synergistic effect of chlorine and UVA has been shown earlier, and for example, chlorine oxide and UVA combination has been used for efficient cleaning and disinfection of drinking water.<sup>47</sup> In order to neutralize the background antibacterial effect of wet rubbed matrix alone surfaces, Na-thiosulphate that has been shown to efficiently neutralize chlorine and other halogens was added to the tests with W surfaces. Indeed, the addition of Na-thiosulphate efficiently removed the antibacterial effect of wet rubbed surfaces (Fig. S5).

Compared with untreated ZnO-based surface coatings, a clear increase in antibacterial activity was observed after abrasive treatment both, under UVA as well as in the dark (Fig. 5). This finding coincides well with topological changes of surfaces after abrasion and increased release of Zn. Under UVA, the increased antibacterial activity also coincides with increase in photocatalytic effect, and therefore, we may conclude that under UVA, the mechanism of antibacterial action is elevated release of ZnO particulates or exposure of higher amount of ZnO micro- and nanostructures on surfaces and resulting increase in UVA-induced production or reactive oxygen species. On the other hand, in the dark, such photocatalytic effect does not take place, and instead, antibacterial activity is achieved by leaching of Zn ions from either surface-released or surface-exposed ZnO structures. Interestingly, after dry or wet rubbing, antibacterial activity did not increase, but on the contrary, decreased (Fig. 5). This finding is somewhat similar to photocatalytic activity where D and W treatments did not enhance the photocatalytic effect, except W-treated ZnO(s) surface. However, unlike in the case of antibacterial results, no significant decrease in photocatalytic effect on D- and W-treated surfaces was observed. The decrease in antibacterial effect after dry and wet rubbing was most prominent in the case of ZnO(c) surface coatings where under UVA illumination, D treatment decreased antibacterial effect by 1.7 and W treatment by 1.5 log<sub>10</sub> (Fig. 5c). Around one log<sub>10</sub> decrease in antibacterial activity was observed also due to W treatment of ZnO(c) surface (Fig. 5c). The exact reason for decreased antibacterial activity due to dry and wet rubbing of surfaces is unknown but we suggest

that the matrix material released during D and W treatments masked the surfaces from bacteria, which were deposited to surfaces in very low liquid volumes.

In summary, our results indicated that relatively mild treatments of acrylic matrix-immobilized ZnO-based coatings may rather decrease the antibacterial activity of such surfaces, while more aggressive treatment involving abrasion is likely to restore and even increase the antibacterial activity. Also earlier studies have suggested that different surface treatment procedures may affect the antibacterial activity differently. While simple rinsing of surfaces and their immersion in water between antibacterial tests, or even wiping with soap solution did not affect antibacterial activity, abrasive treatment of surface-deposited surface coatings decreased the antibacterial effect of some surfaces.<sup>19,23,24,26</sup> However, the extent of antibacterial activity loss has been shown to be dependent on the strength of attachment of the antimicrobial material to surfaces. Therefore, usually polymer or ceramic-embedded surface coatings have been relatively resistant to treatments that involve abrasion and therefore, could be considered durable over time and towards various treatments.<sup>25,28,29,48</sup> Based on our results, however, in the case of matrix-immobilized antimicrobial material, a more aggressive cleaning or abrasion step would be required from time to time, in order to expose the active material to surface and ensure the antibacterial effect.

## Conclusions

The results of our study demonstrated that wear and tear of antimicrobial surface coatings may significantly affect the performance of antimicrobial surfaces. Dry rubbing, wet rubbing, and abrasive treatment, used as simulated wear scenarios for ZnO-based surface coatings, affected the physical appearance of those coatings at the microscale. A significant amount of material was released from surfaces due to aggressive abrasive treatment but a certain amount of surface material was also released during dry and wet rubbing. According to photocatalytic and antibacterial activity assessment, this released material was either acrylic matrix with embedded ZnO in the case of abrasive treatment, or mostly matrix material in the case of dry and wet rubbing. The abrasion-released ZnO resulted in higher photocatalytic activity and increased antibacterial efficacy, supposedly due to light-induced reactive oxygen species production on released ZnO material under UVA illumination and dissolution of antibacterial levels of Zn ions in the dark. The fact that dry and wet rubbing did not increase the antimicrobial activity of ZnO-based surfaces but with the exception of wet rubbing of one of the surface types rather decreased the antimicrobial activity, suggests that matrix material that was released during rubbing, was masking the antimicrobial effect. Therefore, our findings show that dry and wet rubbing of ZnO-based surface coatings performed following the guidance of

US EPA retained the photocatalytic activity of the surfaces but generally decreased the antimicrobial efficacy of those surfaces over a model 4-week use claim. Aggressive abrasion, however, significantly increased both photocatalytic and antibacterial effect. Although such an increased activity may result in positive outcome in short term, during long term and repeated use, it may clearly lead to decomposition of the surface coatings. Therefore, we suggest that a preferred method of preservation or even increasing the antimicrobial activity involves production of relatively “thick” surface coatings in the case of which repeated removal of topmost layers would be possible. Overall, our study emphasizes a clear need for detailed guidelines on cleaning procedures to be applied on antimicrobial surfaces in order to assure their maximal lifetime and performance.

**Acknowledgements** Ülis Sõukand from Estonian Environmental Research Center is thanked for his help with methods of chemical analysis. Estonian Research Council projects COVSG2 and PRG1496 and European Commission project STOP (Grant agreement ID: 101057961) are thanked for their financial support. The research was partly conducted using the NAMUR+ core facility funded by project TT13 “Center of nanomaterials technologies and research (NAMUR+).”

**Data availability** The data supporting the results present in this study can be found in Raw data file submitted as a Supplementary information.

**Conflict of interest** The authors declare that they have no conflict of interest.

**Open Access** This article is licensed under a Creative Commons Attribution 4.0 International License, which permits use, sharing, adaptation, distribution and reproduction in any medium or format, as long as you give appropriate credit to the original author(s) and the source, provide a link to the Creative Commons licence, and indicate if changes were made. The images or other third party material in this article are included in the article’s Creative Commons licence, unless indicated otherwise in a credit line to the material. If material is not included in the article’s Creative Commons licence and your intended use is not permitted by statutory regulation or exceeds the permitted use, you will need to obtain permission directly from the copyright holder. To view a copy of this licence, visit <http://creativecommons.org/licenses/by/4.0/>.

## References

- Cobrado, L, Silva-Dias, A, Azevedo, MM, Rodrigues, AG, “High-Touch Surfaces: Microbial Neighbours at Hand.” *Eur. J. Clin. Microbiol. Infect. Dis.*, **36** (11) 2053–2062 (2017)
- Weber, DJ, Rutala, WA, Miller, MB, Huslage, K, Sickbert-Bennett, E, “Role of Hospital Surfaces in the Transmission of Emerging Health Care-Associated Pathogens: Norovirus, *Clostridium difficile*, and *Acinetobacter* Species.” *Am. J. Infect. Control*, **38** (5) S25–S33 (2010)
- Kundrapu, S, Sunkesula, V, Jury, LA, Sitzlar, BM, Donskey, CJ, “Daily Disinfection of High-Touch Surfaces in Isolation Rooms to Reduce Contamination of Healthcare Workers’ Hands.” *Infect. Control Hosp. Epidemiol.*, **33** (10) 1039–1042 (2012)
- Cassidy, SS, Sanders, DJ, Wade, J, Parkin, IP, Carmalt, CJ, Smith, AM, Allan, E, “Antimicrobial Surfaces: A Need for Stewardship?” *PLoS Pathog.*, **16** (10) e1008880 (2020)
- Redfern, J, Tucker, J, Simmons, L, Askew, P, Stephan, I, Verran, J, “Environmental and Experimental Factors Affecting Efficacy Testing of Nonporous Plastic Antimicrobial Surfaces.” *Methods Protoc.*, **1** (4) 36 (2018)
- Cunliffe, AJ, Askew, PD, Stephan, I, Iredale, G, Cosmans, P, Simmons, LM, Verran, J, Redfern, J, “How Do We Determine the Efficacy of an Antibacterial Surface? A Review of Standardised Antibacterial Material Testing Methods.” *Antibiotics*, **10** (9) 1069 (2021)
- Muller, MP, MacDougall, C, Lim, M, Armstrong, I, Bialachowski, A, Callery, S, Ciccotelli, W, Cividino, M, Dennis, J, Hota, S, Garber, G, Johnstone, J, Katz, K, McGeer, A, Nankooosingh, V, Richard, C, Vearncombe, M, “Antimicrobial Surfaces to Prevent Healthcare-Associated Infections: A Systematic Review.” *J. Hosp. Infect.*, **92** (1) 7–13 (2016)
- Colin, M, Klingelschmitt, F, Charpentier, E, Josse, J, Kanagaratnam, L, De Champs, C, Gangloff, S, “Copper Alloy Touch Surfaces in Healthcare Facilities: An Effective Solution to Prevent Bacterial Spreading.” *Materials*, **11** (12) 2479 (2018)
- Salgado, CD, Sepkowitz, KA, John, JF, Cantey, JR, Attaway, HH, Freeman, KD, Sharpe, PA, Michels, HT, Schmidt, MG, “Copper Surfaces Reduce the Rate of Healthcare-Acquired Infections in the Intensive Care Unit.” *Infect. Control Hosp. Epidemiol.*, **34** (5) 479–486 (2013)
- Kaur, H, Rosenberg, M, Kook, M, Danilian, D, Kisand, V, Ivask, A, “Antibacterial Activity of Solid Surfaces is Critically Dependent on Relative Humidity, Inoculum Volume and Organic Soiling.” *bioRxiv*, 2023.03.28.534510 (2023)
- Adlhart, C, Verran, J, Azevedo, NF, Olmez, H, Keinänen-Toivola, MM, Gouveia, I, Melo, LF, Crijns, F, “Surface Modifications for Antimicrobial Effects in the Healthcare Setting: A Critical Overview.” *J. Hosp. Infect.*, **99** (3) 239–249 (2018)
- Gomes, IB, Simões, M, Simões, LC, “Copper Surfaces in Biofilm Control.” *Nanomaterials*, **10** (12) 2491 (2020)
- Müller, DW, Löblein, S, Terriac, E, Brix, K, Siems, K, Moeller, R, Kautenburger, R, Mücklich, F, “Increasing Antibacterial Efficiency of Cu Surfaces by Targeted Surface Functionalization via Ultrashort Pulsed Direct Laser Interference Patterning.” *Adv. Mater. Interfaces*, **8** (5) 2001656 (2021)
- Cloutier, M, Mantovani, D, Rosei, F, “Antibacterial Coatings: Challenges, Perspectives, and Opportunities.” *Trends Biotechnol.*, **33** (11) 637–652 (2015)
- Jose, A, Gizdavic-Nikolaidis, M, Swift, S, “Antimicrobial Coatings: Reviewing Options for Healthcare Applications.” *Appl. Microbiol.*, **3** (1) 145–174 (2023)
- Calovi, M, Coroneo, V, Palanti, S, Rossi, S, “Colloidal Silver as Innovative Multifunctional Pigment: The Effect of Ag Concentration on the Durability and Biocidal Activity of Wood Paints.” *Prog. Org. Coat.*, **175** 107354 (2023)
- Liu, G, Wu, G, Jin, C, Kong, Z, “Preparation and Antimicrobial Activity of Terpene-Based Polyurethane Coatings



- with Carbamate Group-Containing Quaternary Ammonium Salts.” *Prog. Org. Coat.*, **80** 150–155 (2015)
18. Suzuki, S, Ando, E, “Abrasion of Thin Films Deposited onto Glass by the Taber Test.” *Thin Solid Films*, **340** (1–2) 194–200 (1999)
  19. Cui, J, Shao, Y, Zhang, H, Zhang, H, Zhu, J, “Development of a Novel Silver Ions-Nanosilver Complementary Composite as Antimicrobial Additive for Powder Coating.” *Chem. Eng. J.*, **420** 127633 (2021)
  20. Yin, B, Hua, X, Fan, F, Qi, D, Han, K, Hou, Y, Hou, D, “A Functional and Robust Super-Hydrophobic PCC Coating Based on the Induced Assembly of Modified Zirconium Phosphate.” *J. Appl. Polym. Sci.*, **140** (6) e53427 (2023)
  21. Sutar, RS, Kalel, PJ, Latthe, SS, Kumbhar, DA, Mahajan, SS, Chikode, PP, Patil, SS, Kadam, SS, Gaikwad, VH, Bhosale, AK, Sadasivuni, KK, Liu, S, Xing, R, “Superhydrophobic PVC/SiO<sub>2</sub> Coating for Self-Cleaning Application.” *Macromol. Symp.*, **393** (1) 2000034 (2020)
  22. Lu, Y, Sathasivam, S, Song, J, Crick, CR, Carmalt, CJ, Parkin, IP, “Robust Self-Cleaning Surfaces that Function When Exposed to Either Air or Oil.” *Science (1979)*, **347** (6226) 1132–1135 (2015)
  23. Rosenberg, M, Visnapuu, M, Saal, K, Danilian, D, Pärna, R, Ivask, A, Kisand, V, “Preparation and Characterization of Photocatalytically Active Antibacterial Surfaces Covered with Acrylic Matrix Embedded Nano-ZnO and Nano-ZnO/Ag.” *Nanomaterials*, **11** (12) 3384 (2021)
  24. Bedi, RS, Cai, R, O’Neill, C, Beving, DE, Foster, S, Guthrie, S, Chen, W, Yan, Y, “Hydrophilic and Antimicrobial Ag-Exchanged Zeolite a Coatings: A Year-Long Durability Study and Preliminary Evidence for Their General Microbicidal Efficacy to Bacteria, Fungus and Yeast.” *Microporous Mesoporous Mater.*, **151** 352–357 (2012)
  25. Sahin, F, Sahin, GD, Ceylan, A, Onses, MS, “Highly Durable Antibacterial Surface Through In-situ Grown Copper Nanoparticles for Biomedical Applications.” In: *2022 Medical Technologies Congress (TIPTEKNO)*, pp. 1–4 (2022)
  26. Buhl, S, Peter, J, Stich, A, Brückner, R, Bulitta, C, “Durability and Stability of Antimicrobial Coated Surfaces.” *Curr. Dir. Biomed. Eng.*, **6** (3) 298–300 (2020)
  27. ASTM-D5402, “Standard Practice for Assessing the Solvent Resistance of Organic Coatings Using Solvent Rubs.” (2019)
  28. Bedard, J, Caschera, A, Foucher, DA, “Access to Thermally Robust and Abrasion Resistant Antimicrobial Plastics: Synthesis of UV-Curable Phosphonium Small Molecule Coatings and Extrudable Additives.” *RSC Adv.*, **11** (10) 5548–5555 (2021)
  29. Yang, J, Qian, H, Wang, J, Ju, P, Lou, Y, Li, G, Zhang, D, “Mechanically Durable Antibacterial Nanocoatings Based on Zwitterionic Copolymers Containing Dopamine Segments.” *J. Mater. Sci. Technol.*, **89** 233–241 (2021)
  30. Qian, H, Liu, W, Chang, W, Hao, X, Zhang, D, “D-Cysteine Functionalized Superhydrophobic Nanocomposite Coating with Multiple-Action Antibacterial Property and Enhanced Mechanical Durability.” *Coatings*, **12** (8) 1158 (2022)
  31. EPA, “EPA. 2021. Interim Method for Evaluating the Efficacy of Antimicrobial Surface Coatings.” (2021)
  32. Calfee, MW, Ryan, SP, Abdel-Hady, A, Monge, M, Aslett, D, Touati, A, Stewart, M, Lawrence, S, Willis, K, “Virucidal Efficacy of Antimicrobial Surface Coatings Against the Enveloped Bacteriophage Φ6.” *J. Appl. Microbiol.*, **132** (3) 1813–1824 (2022)
  33. Visnapuu, M, Rosenberg, M, Truska, E, Nõmmiste, E, Šutka, A, Kahru, A, Rähn, M, Vija, H, Orupõld, K, Kisand, V, Ivask, A, “UVA-Induced Antimicrobial Activity of ZnO/Ag Nanocomposite Covered Surfaces.” *Colloids Surf. B Biointerfaces*, **169** 222–232 (2018)
  34. van Oss, CJ, “Acid–Base Interfacial Interactions in Aqueous Media.” *Colloids Surf. A Physicochem. Eng. Asp.*, **78** 1–49 (1993)
  35. Schneider, CA, Rasband, WS, Eliceiri, KW, “NIH Image to ImageJ: 25 Years of Image Analysis.” *Nat. Methods*, **9** (7) 671–675 (2012)
  36. Law, K-Y, “Definitions for Hydrophilicity, Hydrophobicity, and Superhydrophobicity: Getting the Basics Right.” *J. Phys. Chem. Lett.*, **5** (4) 686–688 (2014)
  37. ISO, “ISO 17294-2:2016: Water Quality—Application of Inductively Coupled Mass Spectrometry (ICP-MS)—Part 2: Determination of Selected Elements Including Uranium Isotopes.” (2016)
  38. Oh, S-R, Kim, J-K, Lee, M-J, Choi, K, “Dechlorination with Sodium Thiosulfate Affects the Toxicity of Wastewater Contaminated with Copper, Cadmium, Nickel, or Zinc.” *Environ. Toxicol.*, **23** (2) 211–217 (2008)
  39. ISO, “ISO 22196:2011 Measurement of Antibacterial Activity on Plastics and Other Non-porous Surfaces.” (2011)
  40. Zuccheri, T, Colonna, M, Stefanini, I, Santini, C, Gioia, D, “Bactericidal Activity of Aqueous Acrylic Paint Dispersion for Wooden Substrates Based on TiO<sub>2</sub> Nanoparticles Activated by Fluorescent Light.” *Materials*, **6** (8) 3270–3283 (2013)
  41. Huang, X, Rao, W, Chen, Y, Ding, W, Zhu, H, Yu, M, Chen, J, Zhang, Q, “Infrared Emitting Properties and Environmental Stability Performance of Aluminum/Polymer Composite Coating.” *J. Mater. Sci. Mater. Electron.*, **27** (6) 5543–5548 (2016)
  42. Han, J, Liu, Y, Singhal, N, Wang, L, Gao, W, “Comparative Photocatalytic Degradation of Estrone in Water by ZnO and TiO<sub>2</sub> Under Artificial UVA and Solar Irradiation.” *Chem. Eng. J.*, **213** 150–162 (2012)
  43. Hochmannova, L, Vytrasova, J, “Photocatalytic and Antimicrobial Effects of Interior Paints.” *Prog. Org. Coat.*, **67** (1) 1–5 (2010)
  44. Vu, TV, Nguyen, TV, Tabish, M, Ibrahim, S, Hoang, THT, Gupta, RK, Dang, TML, Nguyen, TA, Yasin, G, “Water-Borne ZnO/Acrylic Nanocoating: Fabrication, Characterization, and Properties.” *Polymers (Basel)*, **13** (5) 717 (2021)
  45. Sirelkhatim, A, Mahmud, S, Seeni, A, Kaus, NHM, Ann, LC, Bakhori, SKM, Hasan, H, Mohamad, D, “Review on Zinc Oxide Nanoparticles: Antibacterial Activity and Toxicity Mechanism.” *Nanomicro Lett.*, **7** (3) 219–242 (2015)
  46. Blomberg, E, Herting, G, Kuttuva Rajarao, G, Mehtiö, T, Uusinoka, M, Ahonen, M, Mäkinen, R, Mäkitalo, T, Odnevall, I, “Weathering and Antimicrobial Properties of Laminate and Powder Coatings Containing Silver Phosphate Glass Used as High-Touch Surfaces.” *Sustainability*, **14** (12) 7102 (2022)
  47. Chuang, Y-H, Wu, K-L, Lin, W-C, Shi, H-J, “Photolysis of Chlorine Dioxide Under UVA Irradiation: Radical Formation, Application in Treating Micropollutants, Formation of Disinfection Byproducts, and Toxicity Under Scenarios Relevant to Potable Reuse and Drinking Water.” *Environ. Sci. Technol.*, **56** (4) 2593–2604 (2022)
  48. Kim, J, Kim, U, Han, K, Choi, J, “Antibacterial Persistence of Hydrophobically Glazed Ceramic Tiles.” *J. Korean Ceram. Soc.*, **59** (6) 920–928 (2022)

**Publisher’s Note** Springer Nature remains neutral with regard to jurisdictional claims in published maps and institutional affiliations.